JTTEE5 20:243–251
DOI: 10.1007/s11666-010-9596-7
1059-9630/$19.00 © ASM International

Influence of Pre-Heated Al 6061 Substrate Temperature on the Residual Stresses of Multipass Al Coatings Deposited by Cold Spray

Silvano Rech, Andrea Trentin, Simone Vezzù, Jean-Gabriel Legoux, Eric Irissou, and Mario Guagliano

(Submitted April 28, 2010; in revised form October 22, 2010)

In this work, the influence of the substrate temperature on the deposition efficiency, on the coating properties and residual stress was investigated. Pure Al coatings were deposited on Al 6061 alloy substrates using a CGT Kinetics 3000 cold spray system. The substrate temperature was in a range between 20 (room temperature) and 375 °C and was kept nearly constant during a given deposition while all the other deposition parameters were unchanged. The deposited coatings were quenched in water (within 1 min from the deposition) and then characterized. The residual stress was determined by Almen gage method, Modified Layer Removal Method, and XRD in order to identify both the mean coating stress and the stress profile through the coating thickness from the surface to the coating-substrate interface. The residual stress results obtained by these three methods were compared and discussed. The coating morphology and porosity were investigated using optical and scanning electron microscopy.

Keywords aluminum, cold spray, curvature, Modified Layer Removal Method, residual stress, XRD

1. Introduction

Traditionally, thermal spray processes such as flame, arc, plasma, and HVOF are used for deposition of thick coatings (Ref 1). Thick coatings deposited by conventional thermal spray processes may undergo phase transformations, recrystallization, and high oxidation (Ref 1, 2) and may exhibit deformation or high residual stresses induced by thermal coefficient of expansion mismatch (Ref 3). Cold spray deposition is gaining more and more interest in the deposition of thick protective coatings due to the low deposition temperature, low residual stress, porosity, and oxygen content of deposited coatings (Ref 4-6). In particular, the cold spray deposition technique allows applying coatings of pure aluminum, aluminum alloys and composites with thickness up to 1 cm which can be used for the protection and the repair of different aluminum components (Ref 7).

Residual stress plays an important role in the thermal spray process and also in cold spray. A number of factors influence the coating residual stress such as quenching due to cooling of the sprayed material, peening due to the plastic deformation of impacted particles, thermal mismatch resulting from the different thermal expansion coefficients of coating-substrate materials and temperature gradient in multipass deposition processes (Ref 8). In this context, the study of coating residual stress, adhesion, and morphology is of primary importance in order to maximize the deposition efficiency, the coating quality and performance and to determine the limits of applicability of cold spray for those applications.

In a previous work (Ref 9), the distribution and the magnitude of the residual stress of an aluminum coating on an aluminum alloy substrate deposited by cold spray was investigated. In particular, the focus was on the influence of particle velocity and coating thickness on the residual stress. It was demonstrated (Ref 9) that residual stresses in pure aluminum coatings deposited on aluminum alloy substrates are compressive and lower in modulus than 50 MPa, and that the average particle velocity (in the range reported 620-765 m/s) does not induce any noticeable variations of residual stress. Also, it was shown

This article is an invited paper selected from presentations at the 2010 International Thermal Spray Conference and has been expanded from the original presentation. It is simultaneously published in *Thermal Spray: Global Solutions for Future Applications, Proceedings of the 2010 International Thermal Spray Conference*, Singapore, May 3-5, 2010, Basil R. Marple, Arvind Agarwal, Margaret M. Hyland, Yuk-Chiu Lau, Chang-Jiu Li, Rogerio S. Lima, and Ghislain Montavon, Ed., ASM International, Materials Park, OH, 2011.

Silvano Rech, Andrea Trentin, and **Simone Vezzù**, Associazione Civen, Via delle Industrie 12, 30175 Marghera, Italy; **Jean-Gabriel Legoux** and **Eric Irissou**, Industrial Materials Institute (IMI), National Research Council Canada (CNRC-NRC), 75 de Mortagne Boulevard, Boucherville, QC J4B 6Y4, Canada; and **Mario Guagliano**, Politecnico di Milano, Piazza Leonardo da Vinci, 32, 20133 Milan, Italy. Contact e-mail: silvano.rech@civen.org.

that residual stress in aluminum coatings depends on coating thickness. The stress increases with increasing thickness in the range of 0.1-0.4 mm, reaching about 50 MPa for a 0.4-mm thick coating, then the stress is rather constant.

The present study is focused on the evaluation of residual stresses caused by the peening effect in cold-sprayed aluminum coatings deposited on Al 6061 alloy substrates heated and stabilized at five different temperatures (20, 100, 200, 300, and 375 °C). The Almen gage curvature method (Ref 10-12), the Modified Layer Removal Method (MLRM) (Ref 3, 13, 14), and XRD (Ref 4, 15, 16) characterization techniques have been used in order to investigate the stress behavior of the coatings as a function of the pre-heated substrate temperature. High reliability among MLRM, XRD, and Almen gage methods measuring Al coating stresses was reported (Ref 9). Furthermore, the combination of MLRM and diffraction methods with layer removal techniques gave the possibility to obtain the depth stress profiles which are of special interest in the case of coated materials.

2. Experimental Procedure

2.1 Experimental Setup

A gas atomized aluminum powder (purity 99.7%) with a particle size between 11 and 38 μm (Valimet H15) has been used as feedstock material. The depositions were carried out by means of the cold spray system (CGT-Kinetiks 3000, CGT Cold Gas Technology GmbH, Ampfing, Germany) provided with the special polymeric nozzle designed for aluminum powder spraying. The coatings were deposited on Al 6061 alloy Almen strips (76 × 19 × 2 mm) in order to evaluate the residual stress by the curvature method and XRD stress characterization. Also square aluminum (6061 alloy) substrates (25 × 25 × 5.95 mm) were coated to perform MLRM (Fig. 1).

The surfaces of the substrates were grit blasted prior to coating in order to optimize the coating adhesion, the average surface roughness (in all sets of samples) following grit blasting was $Ra = 14.65 \pm 3.63$ μm. The grit blasting was performed on both sides of the samples to compensate for the induced curvature that the grit blasting procedure causes on the substrates.

A set of samples was coated to study the effects of different substrate temperatures (20, 100, 200, 300, and 375 °C) on coating residual stress. For depositing coatings, the samples were mounted on a massive copper support attached to a second stainless steel holder equipped inside with three electrical heaters (3000 W). The temperature was monitored by means of a thermocouple (K-type) inserted into the massive stainless steel holder. Four MLRM square substrates were inserted into the copper holder; otherwise, two Almen strips were fixed in contact with the copper holder surface (Fig. 1). A surface thermocouple was used to measure the actual surface temperature of the substrate and the power of the heater was then adjusted until the desired temperature was reached in a steady-state-regime. In addition, an infrared high-speed camera (Thermacam SC3000) was used to verify the temperature uniformity at the surface of the samples prior to deposition.

The main spray parameters were maintained constant for all deposition sets: the stagnation nitrogen gas temperature and pressure were set at 350 °C and 2.5 MPa, respectively. The distance between nozzle and substrate was 20 mm; the powder flow and carrier gas flow rates were kept constant for all depositions. During the spray deposition, no temperature measurements have been performed. However, it is expected that the actual surface temperature beneath the spray gun when the particles hit

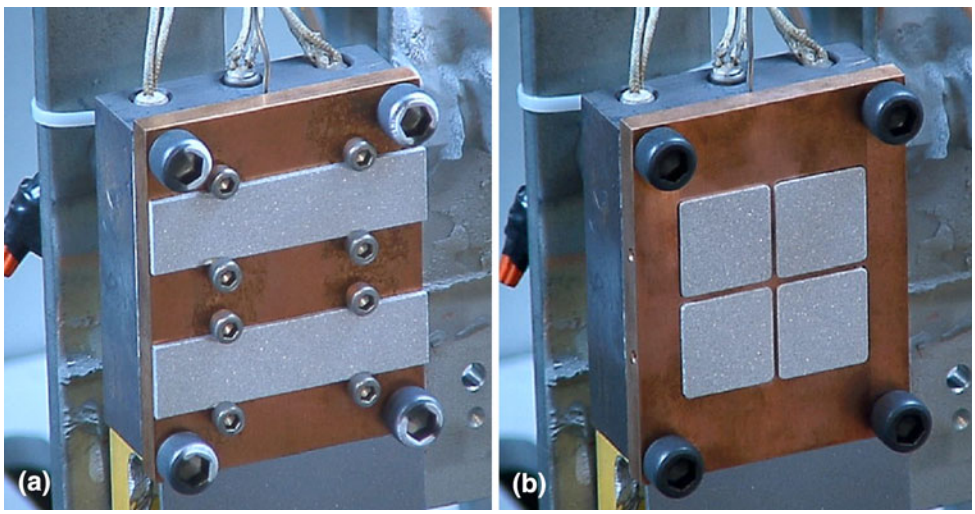

Fig. 1 The samples mounted on a massive copper holder attached on a second stainless steel holder equipped inside with three electrical heaters and a thermocouple. (a) The MLRM square substrates are inserted into the copper holder; (b) the Almen strips are been fixed in contact with the copper holder surface

Table 1 The entire set of sample obtained by cold spray deposition of pure aluminum powder on heated aluminum 6061 substrates; for all samples, the propelling gas temperature and pressure were 350 °C and 2.5 MPa, respectively

Pre-heated substrate temperature, °C	Samples	Number of passes	Coating thickness, μm	Delay for quenching after deposition, s
24	4 MLRM	3	674 ± 54	60
97	4 MLRM	3	695 ± 57	60
198	4 MLRM	2	750 ± 60	60
292	4 MLRM	3	746 ± 60	60
375	4 MLRM	3	820 ± 66	95
24	2 Almen	3	560 ± 45	60
98	2 Almen	3	640 ± 51	60
198	2 Almen	2	454 ± 36	60
292	2 Almen	3	746 ± 60	180
375	2 Almen	3	845 ± 68	180

the substrate is different from the set temperature because of heat exchange due to the high pressure gas stream preheated at 350 °C.

The gun traverse speed was set to 100 mm/s for all experiments and the number of spray passes was set at 2 or 3, in order to have a coating thickness superior to 0.5 mm. The minimum limit for the coating thickness was determined from the dependence of the residual stress inside the aluminum deposit on coating thickness, as reported in our previous study (Ref 9). After the deposition, and in particular in the case of higher-end-temperature deposition conditions (300 and 375 °C), the aluminum coating may partially relax the internal stress if the cooling is performed in air. For this reason, the stress state inside the coatings has been ''frozen'' by quenching of the samples in water (at 20 °C) after deposition. The maximum delay between the deposition and quenching was equal to 180 s. The main characteristics of samples deposited are summarized in Table 1.

To determine the effect of heat treatments on samples having no coating, a set of grit blasted (both sides) Almen samples were heated at the different temperatures (20, 100, 200, 300, and 375 °C) following which they were quenched. In all cases, there was no significant modification in the Almen curvature.

2.2 Metallographic Sample Preparation

The coating microstructure was investigated by means of cross-section light optical microscopy (LOM) (model DM6000M, Leica, Wetzlar, Germany) and scanning electron microscopy (SEM) (model VEGA LMU, TESCAN, Brno, Czechoslovakia). The metallographic samples for coating structure evaluation were cut from sections of both specimens (Almen and MLRM samples) and mounted using an automatic mounting press (MEGAPOL P320, Presi, Grenoble, France). All the samples were sectioned and mounted. Grinding was performed using different grades of abrasive papers and polishing was carried out using diamond suspensions. Final polishing was carried out using 1-μm diamond suspensions. Samples were also chemically etched using modified Keller's reagent (2.5 mL NHO_3, 1.0 mL HCl, 1.5 mL HF, and 95 mL water).

2.3 Image Analysis

The LOM coatings micrographs were processed by Scanning Probe Image Processing (SPIP), analysis software which permits to detect and analyse grains, particles, inclusions, and pores (Ref 17, 18). Five LOM micrographs at 100× and five different LOM micrographs at 200× were processed for every samples.

2.4 Microhardness Depth Profiling

Microhardness measurements on metallographically prepared cross-section samples were also performed. Using a microhardness tester (VMHTAUTO, Leica, Wetzlar, Germany) starting at the coating surface and reaching the substrate using step size of 50 μm, the Vickers 5 g load indentations (three measurements per step) were performed inside every coating.

The average microhardness and the standard deviation of the powder were also reported; 20 indentations (5 g) were performed on a metallographically prepared sample.

2.5 Residual Stress Characterization Techniques

Three different characterization techniques were used for evaluation of the coating residual stresses.

2.5.1 Curvature Method. The curvature method (Almen gage curvature) is widely used to evaluate residual stress in thin coatings (the coating thickness being less than the substrate thickness). The beam theory used in this method was first developed by Stoney (Ref 11) assuming a plane stress state and a constant residual stress distribution over the whole coating thickness. In the case of thicker coatings, other methods were developed more recently also taking into account the coating properties in high-order terms (Ref 19). For the work reported in the present study, the Benabdi-Roche equation has been used because of its higher reliability for thick coatings. The curvature measurements were performed on Almen gage (Model TSP-3, Electronics Inc., Mishawaka IN).

2.5.2 MLR Method. The MLRM allows measuring the dimensional deformation of a substrate after subsequent layer removing by mechanical polishing. Automatic grinding (AbraPol-20, Struers Ltd., Mississauga, Canada) was performed using grit-30 abrasive paper for 15-20 s at 75 N with a rotating speed at 150 rpm. The principle of this characterization is based on measurements of substrate displacements induced by removing a small layer of stressed coating. In this work, the related strains along the surface were measured by a Strain Gage (Vishay CEA-125WT-120/350, Vishay Precision Group, Malvern, PA), recorded by means of a Strain Indicator (Vishay Micro-Measurements mod. P3) and converted via software into the relative stresses according to Kroupa and Rybicki (Ref 3, 13). The measurements were performed with respect to two orthogonal directions, indicated as longitudinal and transverse.

The strain gage was glued on the center of the uncoated side of a sample after cleaning the substrate surface with degreasing agents (the surface should be smooth but not mirror finished) and then the wires were welded onto terminals and protected with a sealant coating to avoid exposure (water, etc.).

2.5.3 XRD Method. The surface and sub-surface layer of material was characterized by measuring the residual stresses by means of a x-ray diffractometer (AST XStress 3000, Stresstech GmbH, Hohn, Germany) (radiation Cr K_α, {311} lattice planes, $2\theta = 139.3°$, V filter, irradiated area of 1 mm^2, $\sin^2\psi$ method, 11 angles of measurement, 30 s of x-ray exposure for each angle). The analytical model adopted to determine the values of the stresses was the one that considers a linear relation between stress and strain and a plane stress condition. The $\sin^2\psi$ method was adopted for determining the results: it assumes a linear relationship between the distance d among the crystal planes and $\sin^2\psi$, whose angular coefficient is used for obtaining the stress value according to Eq 1:

$$\sigma_\phi = \left(\frac{E}{1+\upsilon}\right)_{hkl} \frac{1}{d_{0(hkl)}} \left(\frac{\partial d_{\phi\psi(hkl)}}{\partial \sin^2\psi}\right), \qquad \text{(Eq 1)}$$

where σ is the stress component in an assigned direction, E is the elastic modulus of the material, hkl are the lattice planes (in this case 311), d_0 is the lattice spacing of planes hkl in the undeformed material, ψ is the angle subtended by the bisector of the incident and diffracted XR beam and $\left(\partial d_{\phi\psi(hkl)}/\partial \sin^2\psi\right)$ is the slope of the line d-$\sin^2\psi$. In this formula, the value of the elastic constant used for relating the strain and the stresses is the one of the lattice plane {311}, thus $[E/(1+\nu)]_{311} = 60$ GPa. Equation 1 is valid if the stress components in the direction normal to the surface are null or negligible. In Fig. 2, an example of the d-$\sin^2\psi$ graphs obtained from the measurements is shown. The linear trend is confirmed and the previous assumption confirmed.

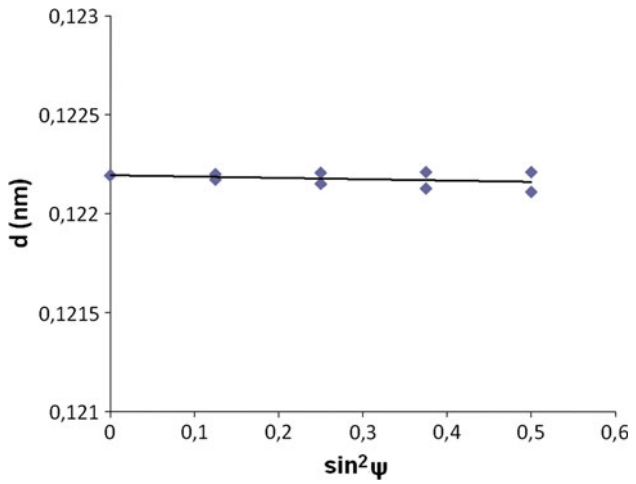

Fig. 2 Example of d-$\sin^2\psi$ graph obtained from a XRD measurement of residual stresses: the slope of the line is used to elaborate the residual stress

For depth stress profiling, step by step removal of thin layers from the surface was required. This operation was performed by using an electro-polishing facility, thus preventing a strong alteration of the pre-existing residual stress state. The measurements were performed with respect to two orthogonal directions.

3. Results and Discussion

3.1 Microstructure and Porosity of Powder

The structure of powder particles observed on SEM images is in a good agreement with the data provided by the manufacturer: the particles are spherical with the presence of some satellites. The microstructure of gas atomized particles is dendritic with the presence of sub-micrometric porosity (Fig. 3b, d).

3.2 Microstructure and Porosity of Coating

No microstructural difference between the two kinds of specimens (Almen and MLRM samples) was observed. In all cases, the coating-substrate interface presents a good interlocking between the impinging Al particles and the Al 6061 substrate, with very low porosity. Consequently, these coatings are well-adhered to Al 6061 substrates, as shown for example in Fig. 3(c).

Figure 3(c) and 3(f) shows aluminum coatings with compact microstructure and the presence of porosity. The pores are prevalently elongated as shown in Fig. 3(f), with intensification in the interface between the passes (white lines of Fig. 3e). For all etched coatings, the microstructure shows no noticeable variations as a function of pre-heating substrate temperature in the range investigated. The dendritic particle microstructure was preserved in the coatings deposited for all substrate temperatures; no recrystallization or grain refinement was observed (Fig. 3d). The particles aspect ratio was found to be close to 0.6-0.8, which clearly indicates that there is no significant difference in deformation level of aluminum particles compared to other cold spray produced aluminum coatings (Ref 9). However, the mechanical interlocking between particles, clearly shown in Fig. 3(d), is an important indication of high particle cohesion.

Porosity area percentage analyses were performed on all coatings and the average porosity and its standard deviation is plotted in Fig. 4 as a function of pre-heated substrate temperature. The porosity is equal to about 2-3% of the coating area and it is rather constant, within the statistical error, for all pre-heated substrates temperatures.

3.3 Microhardness of Powder and Coating

The microhardness data as a function of depth profile are shown in Fig. 5. By evaluating the Vickers indentation profiles, it can be assumed that the hardness is mainly constant along the coating thickness, so the mean coating hardness represents well the average value of the whole data set.

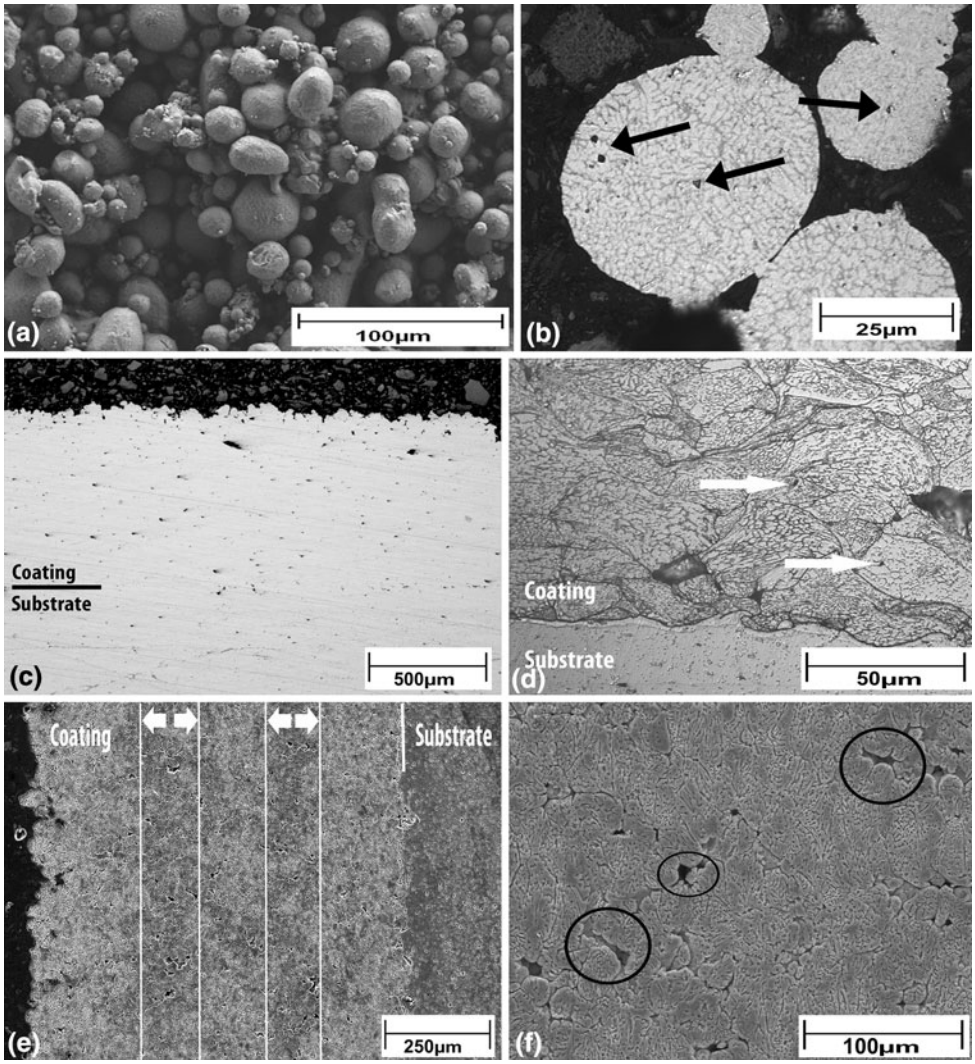

Fig. 3 SEM and LOM micrographs of aluminum powder and aluminum coating on Al 6061 alloy substrate at a pre-heated temperature of 375 °C. (a) Gas atomized Al powder (SEM); (b) Al particle etched (LOM); (c) Al coating on Al 6061 substrate (LOM); (d) etched Al coating (LOM); (e) Al coating on substrate and (f) etched Al coating (SEM). The black arrows point to the pores inside the particles, the black circles identify some elongated pores inside the coating and the larger porosity is prevalently located inside the white lines

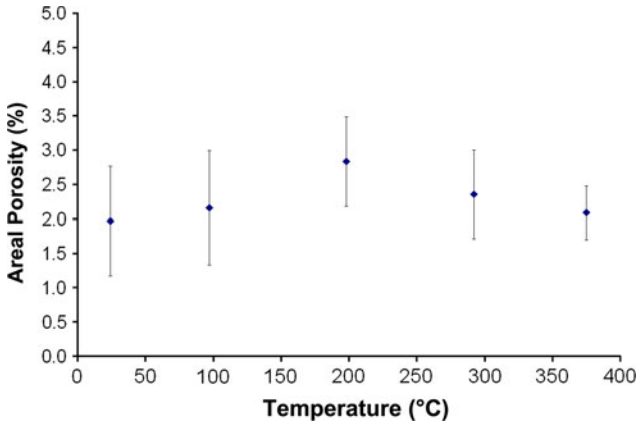

Fig. 4 Coating (% area) porosity of the coating as a function of pre-heated substrate temperature, obtained by image analysis (SPIP)

The microhardness value measured between two adjacent pass is lower than the one measured inside each coating layer because of larger porosity in that area. Figure 6 shows the average Vickers hardness of the aluminum coatings as a function of the pre-heated substrate temperature for every sample. The coating exhibits a microhardness average value of about 50 $HV_{0.005}$, which is independent of substrate temperature for the investigated range (from 24 to 375 °C). These results demonstrate that the coating hardness is about 50% higher than the particle hardness (27.2 ± 4.4 $HV_{0.005}$), which is in a good agreement with the results reported in other works (Ref 6).

3.4 Influence of Substrate Temperature on Residual Stress

The aluminum critical velocity is close to 600 m/s as reported by Schmidt et al. (Ref 20). At this velocity

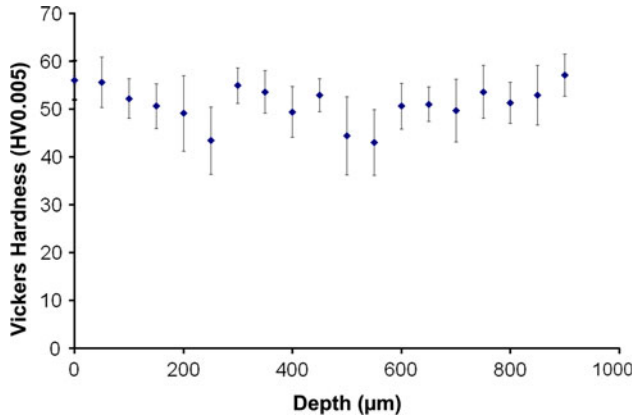

Fig. 5 Vickers microhardness depth profile inside the aluminum coating deposited on Al 6061 alloy substrate at the pre-heated temperature of 375 °C. The error bar reported is the standard deviation of three measurements performed at each depth level

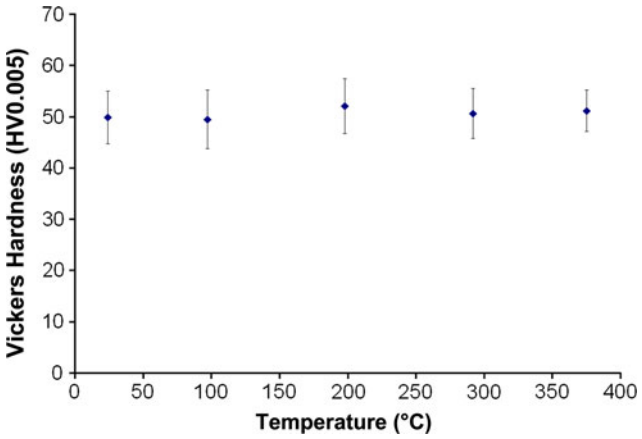

Fig. 6 Average Vickers microhardness as a function of pre-heated substrate temperature. The Vickers microhardness measurements are the average of the depth profiling inside the coating and the bar represents the standard deviation. The microhardness of aluminum powder is 27.2 ± 4.4 $HV_{0.005}$

(Ref 21), both deformation and peening of the impacting particles occur, provoking a compressive stress inside the single-deformed particle and as a consequence also in the whole coating.

The three different stress measurement techniques, namely Almen gage, MLRM, and XRD were adopted to determine the residual stress of the cold spray pure aluminum coatings on thermally stabilized pre-heated Al 6061 substrates. As mentioned before, a previous study (Ref 9) about residual stress of cold spray Al coatings (without substrate pre-heating) showed that the stress was compressive and showed an agreement between the results obtained by the three characterization techniques. It is worth noting that this previous study allowed establishing a procedure in order to have a valid single

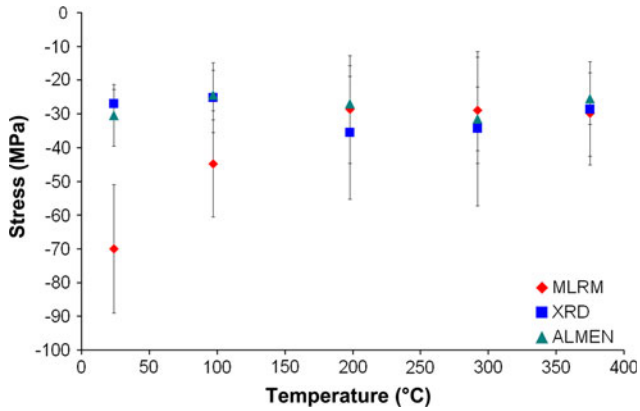

Fig. 7 Residual stresses of pure aluminum coatings evaluated by MLRM, XRD, and Almen gage deposited on Al 6061 alloy substrate as a function of pre-heated substrate temperature

measurement for every coating based on the depth profile measurements. The single points (MLRM and XRD) in Fig. 7 represent the average on the depth profile measurements (longitudinal and transverse). The data arising from the surface measurements (from 0 up to 0.1 mm in the depth profile) were excluded because of the low reliability in the first layer removal (MLRM) and the high coating roughness (XRD). Our previous experiments showed that the residual stress measurement errors were about 30% for MLRM (standard deviation) due to considerable dispersion of the data inside the coatings; about 15-20% for XRD (standard deviation) due to a higher reliability of the technique and lower than 30% for Almen gage mainly arising from the experimental determination of the Almen curvature. Figure 7 shows the measured residual stress as a function of pre-heated substrate temperature. The stress values measured by XRD and Almen gage methods are in agreement and are about 30 MPa, independent of the substrate pre-heating temperature. Contrary to XRD and Almen gage methods, the MLRM method trend shows a residual stress loss in magnitude (mathematical modulus) with increasing pre-heated substrate temperature, starting from 70 MPa at room temperature and reaching 30 MPa at over 200 °C. This trend is compatible with a stress relieving behavior that is a function of the pre-heated substrate temperature.

The samples were quenched in water after a delay of 60-180 s (Table 1) from the end of the cold spray deposition, so it is possible that there was a higher level of stress relaxation at higher temperature (Ref 22, 23). The discrepancy between MLRM and the other two techniques, XRD and Almen gage stress measurements, which exhibit constant stress, can also be attributed to different sample geometry (mainly thickness) and more likely to differences in sample holder configuration and geometry that overall might have induced a different thermodynamic behavior during and after cold spray deposition. Further investigations are in progress to better understand this thermomechanical stress behavior and to evaluate the compressive stress dependency on substrate thickness and on pre-heated substrate temperature.

3.5 MLRM Depth Profile Stress Inside the Coating

Figure 8 shows the stress depth profiles obtained by layer removal methods for the sample deposited on a substrate pre-heated at 375 °C. The measurements were performed with respect to two orthogonal directions. The residual stress is constant along the coating thickness except for the surface layer where no (or very low) peening occurs and inside the coatings, at a depth of about 250 and 600 μm from the coating surface where there are two peaks of tensile stress. Finally, there is a compressive stress intensification on substrate that occurred because of the peening effect of grit blasting and which cannot be distinguished from the (lower) effect due to the peening of cold-sprayed particles. The two tensile peaks are exactly on the interface between subsequent cold spray passes as can be seen on the SEM-graph overlap (Fig. 8).

Johnson et al. (Ref 24) studied the elastic-plastic transition and the energy dissipation of a high velocity (500 m/s) flat-plate projectile (up to 50 mm) impacting on an Al 6061 alloy plate.

They found that after time, on the order of a few tens of microseconds, the mechanical impact energy is transferred to atomic motion (and increased temperature) through normal inelastic properties inherent to all solid metals. The time in which the material is in a dynamic transient, mainly between the elastic-plastic transition and the release from the shocked state, is in the order of a few tens of microseconds. In the case of cold sprayed impinging aluminum particles, this is the time required for lattice rearrangement and dislocation creation in which the particle is in a dynamic evolution.

The average velocity of cold-sprayed aluminum particles with the parameters used in this study is about 650 mm/s (Ref 9, 21). The gun traverse speed was 100 mm/s, the diameter of the spray spot on the substrate was about 10 mm and the single pass deposition thickness was about 250-300 μm. With these conditions, one can calculate that

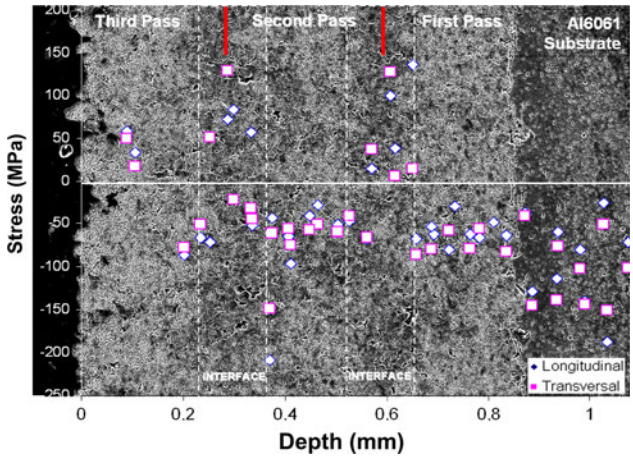

Fig. 8 Depth profile residual stresses evaluated by MLRM. SEM image (etched coating) is superimposed on the stress data. The three passes of pure aluminum cold sprayed coating deposited on Al 6061 alloy substrate (pre-heated at 375 °C) are evident. The larger porosity is located in the area between the dashed lines (interfaces between two adjacent passes)

every particle (25 μm average diameter) inside a single pass coating undergoes several hits from other particles during the time estimate by Johnson, which is the dynamic particle evolution time. This is the time in which the high particle velocity spraying may cause a local plastic deformation resulting in local compressive stresses. A single aluminum layer was deposited on the four MLRM samples (see Fig. 1) in about 50 s, so this time was the delay between two next passes. Because of the delay between two next passes is much larger than the Johnson time (the dynamic particle evolution time), the tensile peak measured at the interface between passes must be examined with a macroscopic view: the aluminum preceding passes (and original substrate) must be considered as a substrate for the next pass. Lyphout et al. (Ref 25) reported a coating/substrate stresses accommodation after spray depositions, this stresses rearrangement were localized in the interface and in the substrate itself, so in the same manner at the interface between the last sprayed pass and the preceding passes, the stress rearrangement take place. In this macroscopic view, the stress peaks at the interface are justified as the balance of the compressive (above all peening) stress inside the next pass coating (Ref 26). These tensile peaks can be seen for all the pre-heated substrate temperatures and no evidence of substrate temperature influence (Fig. 9) was found. Further experiments aimed to better understand this phenomenon are in progress.

Figure 9 also shows a significant stress relief at higher pre-heating temperatures in the surface layer of the substrates: the compressive peaks on substrates (mainly due to the grit blasting peening effect) decrease from about 500 MPa at 24 °C to about 50 MPa at 292 °C. This stress relief on substrates is due to the higher substrate temperature but also to the increasing of the time necessary to reach and stabilize the higher temperature: about 180 s to stabilize the temperature at 97 and 198 °C and about 600 s to stabilize the temperature at 292 and 375 °C.

4. Conclusions

Aluminum coatings were deposited on pre-heated Al 6061 alloy substrates at different temperatures in the 24-375 °C range. The coated samples were quenched in water after a period of no more than 180 s following the deposition. Modified layer removal, x-ray diffraction and Almen gage methods were used to evaluate the residual stresses induced by the deposition process. The influence of pre-heated substrate temperature on coating residual stress was investigated with the three methods. The stress values measured by the XRD and Almen gage methods were in agreement and are about 30 MPa, independent of the substrate pre-heating temperature. The MLRM method results were compressive and evolved from about 70 to 30 MPa as a function of the pre-heated substrate temperature. The discrepancy observed between the MLRM and the two other methods may be attributable to a different stress relaxation, however, it is more likely due to a difference in sample and sample holder geometry.

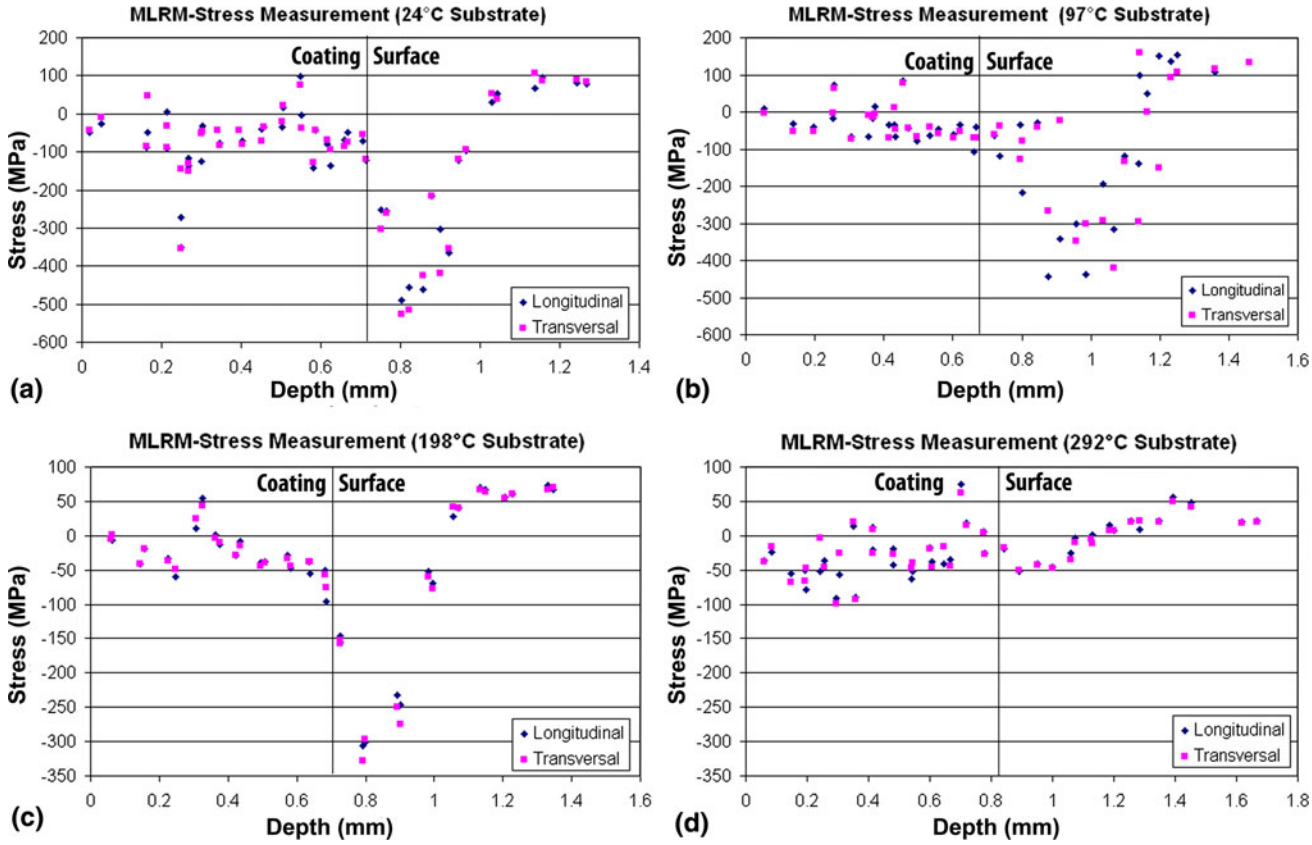

Fig. 9 Depth profile residual stresses evaluated by MLRM. (a) Three pass coating deposited on Al 6061 alloy substrate (pre-heated at 24 °C); (b) three pass coating deposited on Al 6061 alloy substrate (pre-heated at 97 °C); (c) two pass coating deposited on Al 6061 alloy substrate (pre-heated at 198 °C); (d) three pass coating deposited on Al 6061 alloy substrate (pre-heated at 292 °C)

The MLRM depth profile on a multi-pass coating revealed the presence of tensile stress peaks at interfaces between sequential passes. Considering the delay between two next passes, every aluminum passes (and original substrate) must be considered as a substrate for the next pass, therefore, in a macroscopic view the stress peaks located at interfaces arise as the accommodation and balance of the stresses in the same manner of stresses rearrangement between coating and substrate. Further investigations are in progress.

References

1. L. Pawlowski, *Chapter 7—Methods of Coatings' Characterization, Science and Engineering of Thermal Spray Coatings*, 2nd ed., John Wiley & Sons Ltd, New York, 2008, p 291-382
2. S. Deshpande, S. Sampath, and H. Zhang, Mechanisms of Oxidation and its Role in Microstructural Evolution of Metallic Thermal Spray Coatings—Case Study for Ni-Al, *Surf. Coat. Technol.*, 2006, **200**, p 5395-5406
3. F. Kroupa, Residual Stresses in Thick, Non-Homogenous Coating, *J. Therm. Spray Technol.*, 1997, **6**(3), p 147-150
4. J. Pina, A. Dias, and J.L. Lebrun, Study by X-ray Diffraction and Mechanical Analysis of the Residual Stress Generation During Thermal Spraying, *Mater. Sci. Eng. A*, 2003, **347**, p 21-31
5. T.H. Van Steenkiste, J.R. Smith, and R.E. Teets, Aluminum Coatings via Kinetic Spray with Relatively Large Powder Particles, *Surf. Coat. Technol.*, 2002, **154**, p 237-252
6. A. Papyrin, V. Kosarev, S. Klinkov, A. Alkhimov, and V.M. Fomin, *Chapter 5—Current Status of the Cold Spray Process, Cold Spray Technology*, 1st ed., Elsevier Ltd, Amsterdam, 2007, p 249-309
7. V. Champagne, The Repair of Magnesium Rotorcraft Components by Cold Spray, *J. Fail. Anal. Prevent.*, 2008, **8**(2), p 164-175
8. R. Molz, A. Valarezo, and S. Sampath, Comparison of Coating Stresses Produced by High Velocity Liquid/Gas Fuel and Triplex Pro200 Plasma Guns Using in situ Coating Stress Measurement, *International Thermal Spray Conference & Exposition 2008: Thermal Spray Crossing Borders*, 2-4 June 2008 (Maastricht, Holland), ASM International, 2008, p 461-466
9. S. Rech, A. Trentin, S. Vezzù, E. Irissou, J.G. Legoux, B. Arsenault, M. Lamontagne, C. Moreau, and M. Guagliano, Characterization of Residual Stresses in Al and Al/Al2O3 Cold Sprayed Coatings, *International Thermal Spray Conference & Exposition 2009: Expanding Thermal Spray Performance to New Markets and Applications*, 4-7 May 2009 (Las Vegas, Nevada), ASM International, 2009, p 1012-1017
10. M. Guagliano, Relating Almen Intensity to Residual Stresses Induced by Shot Peening: A Numerical Approach Stresses in Thick, Non-Homogenous Coating, *J. Mater. Proc. Technol.*, 2001, **110**, p 277-286
11. G.G. Stoney, The Tension of Metallic Films Deposited by Electrolysis, *Proc. R. Soc. Lond.*, 1909, **A82**, p 172-175
12. D.S. Rickerby and P.J. Burnett, Correlation of Process and System Parameters with Structure and Properties of Physically Vapour-Deposited Hard Coatings, *Thin Solid Films*, 1988, **157**, p 195-222
13. E.F. Rybicki, R.T.R. McGrann, and J.R. Shadley, Applications and Theory of the Modified Layer Removal Method for the Evaluation of Through-Thickness Residual Stresses in Thermal

Spray Coated Materials, *The Fifth International Conference on Residual Stresses*, ICRS-5, 16-18 June 1997 (Linköping, Sweden), p 994-999
14. Modified Layer Removal Method for Evaluating Residual Stresses in Thermal Spray Coatings, Accepted Practice for Mechanical Properties, # 1-AP MP001-02, ASM International Thermal Spray Society, January 2002
15. M. Guagliano, A Numerical Model to Investigate the Role of Residual Stresses on the Mechanical Behavior of Al/Al_2O_3 Particulate Composites, *J. Mater. Eng. Perform.*, 1998, **7**(2), p 183-189
16. T.C. Totemeier and J.K. Wright, Residual Stress Determination in Thermally Sprayed Coatings—A Comparison of Curvature Models and X-ray Techniques, *Surf. Coat. Technol.*, 2006, **200**, p 3955-3962
17. S. Rech, A. Trentin, V. Stoyanova, and S. Vezzù, Study of Copper and Copper/Alumina Coldsprayed Deposits, *International Thermal Spray Conference & Exposition 2008: Thermal Spray Crossing Borders*, 2-4 June 2008 (Maastricht, Holland), ASM International, 2008, p 1197-1201
18. Grain Analysis, User's and Reference Guide, Version 4.4, Scanning Probe Image Processor, Image Metrology, 2008, p 163-189
19. M. Benabdi and A. Roche, Mechanical Properties of Thin and Thick Coatings Applied to Various Substrates, Part I, An Elastic Analysis of Residual Stresses Within Coating Materials, *J. Adhes. Sci. Technol.*, 1997, **11**(2), p 281-299
20. T. Schmidt, F. Gartner, H. Assadi, and H. Kreye, Development of a Generalized Parameter Cold Spray Deposition, *Acta Mater.*, 2006, **54**, p 729-742
21. H. Fukanuma, N. Ohno, B. Sun, and R. Huang, In-Flight Particle Velocity Measurements with DPV-2000 in Cold Spray, *Surf. Coat. Technol.*, 2006, **201**(5), p 1935-1941
22. S. Kuroda and T.W. Klyne, The Quenching Stress in Thermally Sprayed Coatings, *Thin Solid Films*, 1991, **200**, p 49-66
23. Y.C. Fung, *Chapter 12—Elasticity and Thermodynamics, Foundations of Solid Mechanics*, Prentice-Hall International, Englewood Cliffs, NJ, 1965, p 353-402
24. J.N. Johnson, R.S. Hixson, and G.T. Gray, III, Impact Loading of an Aluminum/Alumina Composite, *J. Phys. IV France*, 1994, **4**(C8), p 325-330
25. C. Lyphout, P. Nylén, A. Manescu, and T. Pirling, Residual Stresses Distribution through Thick HVOF Sprayed Inconel 718 Coatings, *J. Therm. Spray Technol.*, 2008, **17**(5-6), p 915-923
26. Y.C. Tsui and T.W. Clyne, An Analytical Model for Predicting Residual Stress in Progressively Deposited Coatings. Part 1: Planar Geometry, *Thin Solid Films*, 1997, **306**, p 23-33